Molecular Dynamics Simulations of the Properties of Cosolvent Solutions

Rajappa Chitra and Paul E. Smith*

Department of Biochemistry, Kansas State University, Manhattan, Kansas 66506-3702

Received: February 11, 2000; In Final Form: April 6, 2000

The physical and dynamical properties of sodium chloride, guanidinium chloride, urea, and 2,2,2-trifluoroethanol solutions have been investigated as a function of cosolvent concentration using molecular dynamics simulations. Properties studied included: solution densities, radial distribution functions and coordination numbers, diffusion constants, residence and reorientational times, and dielectric properties. In most cases, the observed trends in the experimental data as a function of increasing concentration were well reproduced. However, quantitative agreement with experiment was relatively poor, with most cosolvent effects being exaggerated in the simulations. The results highlight significant differences as well as similarities between the effects of guanidinium chloride and urea cosolvents. Aggregation of 2,2,2-trifluoroethanol molecules in water at higher concentrations was also observed, in agreement with experiment.

Introduction

For over 100 years cosolvents have been known to affect the structure and thermodynamics of biological molecules. A knowledge of the mode of action of many cosolvents would be extremely useful for the understanding of processes such as protein folding, macromolecular assembly, DNA-protein interactions, etc. Even so, a clear understanding of the exact nature of these cosolvent effects remains elusive.[1−6] Recently, molecular simulations have been used to complement experimental studies and have provided additional information concerning the interaction of cosolvents with peptides at the atomic level,[7−9] and the effects of cosolvents on the hydration of hydrophobic solutes.[10] However, such computational studies are only as reliable as the force fields used to describe the interactions between different components of the solution.

Current force fields are typically designed to reproduce experimental data for pure solutions. Unfortunately, cosolvent effects result from the interaction of biomolecules with a solution containing several species. Therefore, it is typically assumed that the force fields developed for two individual pure solutions, water and TFE for example, will adequately describe any mixture of TFE and water using standard parameter combining rules. In addition, the partial atomic charges used to describe electrostatic interactions are effective charges which implicitly include any polarization effects present in the pure solutions. It is not clear whether these effective charges give a realistic representation of polarization effects for solution mixtures. In this paper we begin to investigate the validity of some of these assumptions and determine the properties of common cosolvent solutions as described by current force fields.

We have chosen to study aqueous solutions of sodium chloride, urea, guanidinium chloride (GdmCl), and 2,2,2-trifluoroethanol (TFE) using molecular dynamics simulations to investigate the properties of these solutions as a function of cosolvent concentration. These cosolvent solutions exhibit a range of physical and thermodynamic properties which are often dependent on the particular ratio of cosolvent to solvent.[2] The solution properties have been investigated in detail and compared with the corresponding experimental properties where possible. An indication of the strengths and weaknesses of present force fields is essential for the study of cosolvent effects via computational techniques.

To our knowledge very few computational studies of this kind have been performed. There have been several studies of the effects of sodium chloride concentration on the solution properties of water molecules and ions,[11−14] and individual studies of urea at different concentrations,[15−20] but no systematic studies of urea, guanidinium chloride, or TFE solutions. Obviously, there are many water models and several different force fields for urea and TFE present in the literature. However, a comparison of all the models would be implausible. Therefore, we have chosen to confine our studies to the SPC/E model for water[21] and cosolvent parameters obtained from the more common force fields available at present. This approach should provide a reasonable indication as to the general validity of current descriptions of cosolvent solutions.

Methods

Classical molecular dynamics techniques were used to simulate the different solutions reported here. Table 1 lists the force field parameters used,[21−25] all of which were taken from the current literature. Intramolecular parameters were taken from the same source where possible, or from the CHARMM22 force field[26] for analogous compounds. Initial configurations of the different solutions were generated from a cubic box ($L \approx 2.5$ nm) of 512 equilibrated water molecules by randomly replacing waters with cosolvent, until the required concentration was attained. Minimization was carried out with 100 steps of steepest descent, which was followed by extensive equilibration. Initial equilibration of the system was performed for 1 ns. The equilibration was then continued until all interspecies potential energy contributions displayed no drift with time. Simulations were performed in the N, p, T ensemble at 300 K and 1 atm using the weak coupling technique[27] to modulate the temperature and pressure, with relaxation times of 0.1 and 0.5 ps, respectively. SHAKE[28] was used to constrain all bonds with a relative tolerance of 10^{-4}, allowing a 2 fs time step for integration of

* To whom correspondence should be addressed. Fax: 785-532-7278. Email: pesmith@ksu.edu.

10.1021/jp000558t CCC: $19.00
Published on Web 05/27/2000

TABLE 1: Nonbonded Force Field Parameters[a]

species	atom	q, |e|	ϵ, kJ/mol	σ, nm	ref
H_2O	O	−0.8476	0.6506	0.3166	21
	H	0.4238	0.0		
Na^+	Na	1.0000	0.2340	0.2850	22
Gdm^+	N	−0.8000	0.7113	0.3250	23
	C	0.6400	0.2092	0.2250	
	H	0.4600	0.0		
Cl^-	Cl	−1.0000	0.5380	0.3750	22
urea	C	0.1420	0.4393	0.3750	24
	O	−0.3900	0.8786	0.2960	
	N	−0.5420	0.7113	0.3250	
	H	0.3330	0.0		
TFE	CH_2[b]	0.2600	0.4896	0.3920	25
	CF_3	0.5900	0.4059	0.3361	
	O	−0.5500	0.8496	0.2955	
	F	−0.2000	0.5538	0.3050	
	H	0.3000	0.0		

[a] Symbols are q, atomic charge; ϵ and σ, Lennard-Jones 6−12 well depth and diameter, respectively. The geometric mean was used for both ϵ and σ combining rules. [b] United atom carbons.

TABLE 2: Summary of the Molecular Dynamics Runs[a]

cosolvent	T_{sim} (ns)	N_c	N_w	$\langle V\rangle$ (nm^3)	C_c (mol/L)	ρ^{MD} (g/cm^3)	ρ^{exp} (g/cm^3)
none	2	0	512	15.411	0.00	0.9937(9)	0.997[b]
NaCl	2	5	502	15.120	0.55	1.0251(7)	1.019
NaCl	4	9	494	14.928	1.00	1.0483(6)	1.037
NaCl*	2	18	988	29.871	1.00	1.0478(9)	1.037
NaCl	2	14	484	14.688	1.58	1.078(1)	1.058
NaCl	2	18	476	14.532	2.06	1.0999(8)	1.076
GdmCl	3	9	494	15.635	0.96	1.036(1)	1.021
GdmCl	2	30	410	15.117	3.30	1.126(2)	1.075
GdmCl	3	50	350	15.343	5.41	1.199(2)	1.120
urea	3	9	503	15.798	0.95	1.0091(5)	1.012
urea	2	50	400	15.641	5.31	1.0836(5)	1.078
urea	2	75	350	15.959	7.80	1.1246(8)	1.113
TFE	2	9	476	15.352	0.97	1.0248(5)	1.031
TFE	2	25	420	15.566	2.67	1.0738(3)	1.085
TFE	2.5	40	360	15.603	4.26	1.116(1)	1.137
TFE*	1	110	988	42.723	4.28	1.1194(3)	1.137
TFE	2	225	0	27.023	13.82	1.383(1)	1.381

[a] N_c, number of cosolvent molecules; N_w, number of water molecules; $\langle V\rangle$, average volume of the solution; C_c, cosolvent concentration; T_{sim}, total simulation time. ρ^{MD} and ρ^{exp} are the simulated and experimental densities, respectively. * indicates a cosolvent concentration repeated with a larger box length. [b] From ref 65. Experimental densities for NaCl, GdmCl, and urea solutions from ref 66, and from ref 55 for TFE. 4.3 M TFE is approximately 30% by volume of TFE. Numbers in parentheses indicate the error in the last digit.

the equations of motion. Total simulation times were in the 1−4 ns range (see Table 2), the final nanosecond of which was used for calculating ensemble averages. The Ewald technique[29] was used to calculate electrostatic interactions. A convergence parameter of 2.5 nm^{-1} was used in combination with a real space cutoff of 1.2 nm and including all lattice vectors with $n^2 \leq 49$. Configurations were saved every 0.1 ps for the calculation of various properties. For the systems simulated here, our code requires 10 min/ps on a DEC Personal Workstation (EV5/600 MHz). For polyatomic solvents and cosolvents, the center of mass was used during analysis to determine the position of the species of interest. Standard deviations were estimated by determining properties from four subaverages spanning 250 ps each. The simulation results are summarized in Table 2.

Residence times of a given species (j) around another species (i) were calculated as follows. At a given configuration, only those molecules (j) within a distance less than the first minimum in the radial distribution function, g_{ij}, were considered to be bound to the species of interest (i). Any molecule j that returned to this coordination shell after escaping for less than a delay time, t_{delay}, was considered to be continuously bound to molecule i. However, when any of the j molecules was out of the coordination shell of i for longer than t_{delay}, it was considered to be a free molecule. In the calculations reported here, t_{delay} was taken to be 1 ps. The first passage time, t_{fpt}, of molecule j around i was defined as the duration of the time for which it was bound to i. That is, this time indicates the duration between transitions when molecule j goes from the bound state to the free state. A series of first passage times was calculated for all molecules j around molecules i using the last nanosecond of the trajectory. These were then arranged in increasing order of magnitude: $t_1 \leq t_2 \leq ... \leq t_k ... \leq t_n$, where n is the total number of transitions from the bound to the free state. It is then possible to construct a Hazard plot using these ordered first passage times and the Cumulative Hazard, defined as follows:[30,31]

$$H_k = \sum_{l=0}^{k-1} \frac{1}{(n-l)}$$

A plot of H_k against the first passage times should be linear for a Poisson process,[32] and was linear for all the processes considered here. The slope of this plot gives the dissociation rate and the residence time of species j around species i.

The dielectric constants, ϵ, of the various solutions were determined from the fluctuation of the total dipole moment, **M**, of the system. In the case of the two salt solutions—NaCl and GdmCl—only the water molecules contributed to the dipole moment, whereas in the case of urea and TFE, the solute molecules also contributed to the dipole moment of the system as a whole. If V and T are the average volume and the temperature of the system, respectively, then (under conducting boundary conditions) the dielectric constant is given by[33]

$$\epsilon = 1 + \frac{\langle \mathbf{M}^2\rangle - \langle \mathbf{M}\rangle^2}{3\epsilon_0 VRT}$$

where R is the gas constant and ϵ_0 is the permittivity of vacuum. When ϵ was plotted against time, after averaging over time origins,[34] the curves exhibited a plateau after an initial increase. The plateau value at 500 ps was taken to be the dielectric constant of the solution. The dielectric relaxation time, τ_M, was calculated from the autocorrelation function, $\langle \mathbf{M}(t)\cdot\mathbf{M}(0)\rangle$ of the total dipole moment of the system. This autocorrelation function typically decays exponentially as e^{-t/τ_M},[35] and produced a good fit for all the solutions except for 3.3 and 5.4 M GdmCl, where there appeared to be more than one relaxation time. For consistency, we report data only for the single-exponential approximation. τ_M was obtained by fitting the normalized autocorrelation function to a single-exponential function using a simple fitting procedure. For Ewald electrostatics with conducting boundary conditions, τ_M is identical to the Debye relaxation time, τ_D.[35]

Molecular reorientations in the first coordination shell (defined by the position of the first minimum in the rdf) were studied by calculating the correlation functions: $\langle P_1(\cos\theta)\rangle$, where $\cos\theta(t) = \mathbf{e}(t)\cdot\mathbf{e}(0)$. P_1 is the first-order Legendre polynomial and **e** represents a unit vector in the molecular coordinate frame. We have calculated the reorientation times for water around positive ions ($\tau^{\mu}_{+,v}$), negative ions ($\tau^{\mu}_{-,v}$) and neutral solutes (listed under $\tau^{\mu}_{+,v}$ for convenience). For all of the above, the unit vector **e** was taken to be along the direction of the water dipole. In addition, we have also calculated these quantities ($\tau^{\mu}_{+,+}$) for reorientation of Gdm^+ around Gdm^+ ions

and for urea around urea. For these calculations, the unit vectors **e** were taken to be along a C−N bond and along the C=O bond, respectively. All these correlation functions were observed to decay exponentially with a relaxation time τ^{μ}.[36]

Local electroneutrality within the solution was monitored as a function of distance by calculating the net charge around a given species in solution. For the salt solutions, this was performed in two ways; (i) taking into account only the ionic species, and (ii) considering water molecules as well as ions. Only the latter method is applicable to the neutral solutions. The net charge is taken to be the product of the charge on the species and the number of such molecules around a given molecule *i*,

$$Q_i(R) = \sum_j q_j \rho_j \int_0^R g_{ij}(r) 4\pi r^2 \, \mathrm{d}r$$

where $g_{ij}(r)$ is the radial distribution function of species *j* around species *i* and ρ_j and q_j are the number density and charge, respectively, of species *j*. When the net charge was calculated using method (ii), it was determined as the total charge density due to all species around the origin. The net charge was calculated to distances beyond $L/2$, where L is the simulation cell edge length, and no periodic images were considered.

Diffusion constants for the different species were calculated from the fluctuation of the position coordinates:

$$Dt = \lim_{t \to \infty} (\langle r^2 \rangle - \langle r \rangle^2)$$

The averages were taken over all the particles as well as over time origins. In all cases, a plot of $\langle r^2 \rangle - \langle r \rangle^2$ against t was linear, and the diffusion coefficient was given by the slope of the plot as estimated between 50 and 150 ps. The diffusion constants determined by the above formula were identical with those calculated from the slope of the mean squared displacement of the particles,[37] but exhibited superior statistics.

Results and Discussion

In this section, a variety of physical properties of NaCl, GdmCl, urea, and TFE solutions are presented as a function of concentration. The concentrations considered here are typical of the range of concentrations over which the cosolvents are used experimentally; GdmCl (6 M), urea (8 M) and TFE (30% v/v). Sodium chloride was also included for comparison. The data for pure TFE was used to help rationalize many of the observed trends, while any possible system size effects were investigated by repeating some simulations using larger system sizes. For convenience, the different species have been denoted as follows: *u*, (neutral) solute; *v*, solvent; +, cations; and −, anions. Also, an asterisk is used to denote a cosolvent concentration that has been repeated using a larger system size.

A. Solution Densities. A comparison of the simulated and experimental densities for the different cosolvent solutions is presented in Table 2 and Figure 1. The density of pure SPC/E water was slightly low compared with the experimental density but is in agreement with previous values,[38] while the density of pure TFE was also very well reproduced. A slight decrease in water density, from the original parametrization using cutoffs, was expected on inclusion of long range electrostatic interactions.[38] This was a minor effect. As Ewald electrostatics are essential for a realistic treatment of ionic systems,[39] they were adopted here to maintain consistency between the simulations. All solution densities increased with addition of the heavier cosolvents. In general, deviations from the experimental values

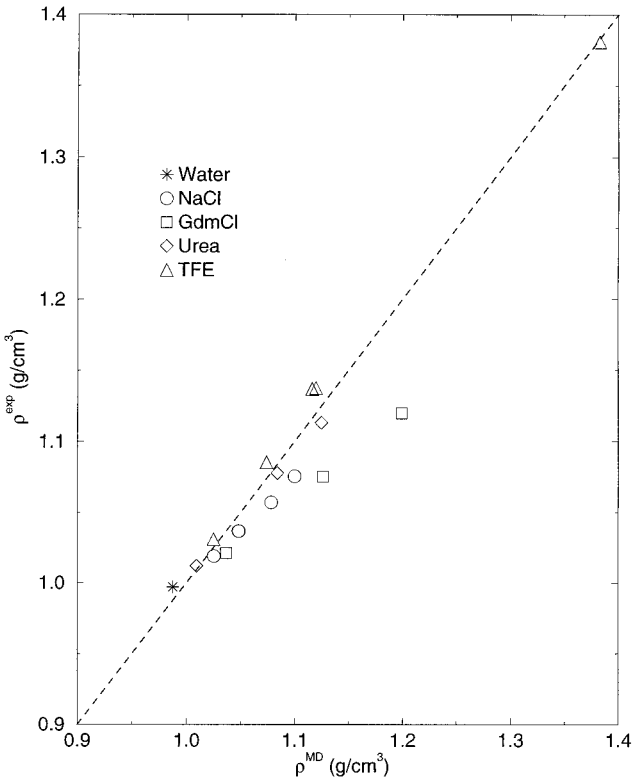

Figure 1. Simulated versus experimental densities of the different cosolvent solutions.

increased with cosolvent concentration over the ranges considered here. Sodium chloride and GdmCl solutions displayed an increasing deviation to higher simulation densities with concentration, with the higher concentration GdmCl solutions differing significantly from the experimental values. It appeared that the parameters associated with the salt solutions were overestimating electrostriction effects in these systems, which could be a result of neglecting explicit polarization effects. Urea also deviated slightly toward higher solution densities but remained in good agreement with experiment. TFE solution densities were reasonable although consistently lower than experiment. System size effects for 1 M NaCl and 4.3 M TFE were negligible. Interestingly, the experimental densities for 6 M GdmCl, 8 M urea, and 30% v/v TFE are very similar (∼1.13 g/cm^3).

B. Radial Distribution Functions. Radial distribution functions (rdfs) between different cosolvent species, as well as those between cosolvent and water, were calculated in order to monitor any change in the structure of the solutions with concentration. Figure 2 shows the rdfs between selected ion pairs, neutral cosolvents, and between water and different cosolvent species. Coordination numbers between different species, N_{ij}, are also shown in Figure 3a as a function of concentration. The positions of the first minimum and the corresponding coordination numbers compare well with other simulation studies.[40−43]

Figure 3a and Table 3 suggest that the solvation of the cations by water was relatively independent of concentration, whereas the neutral solutes became more desolvated. The coordination numbers of water molecules around the chloride ions suggested that they were desolvated to a greater extent at higher concentrations, particularly in GdmCl solutions. Coordination numbers between the different species in TFE solutions indicated an increasing degree of TFE association with concentration, together with decreasing solvation of TFE by water and an increase in water structure (see Figure 2). There was a slight

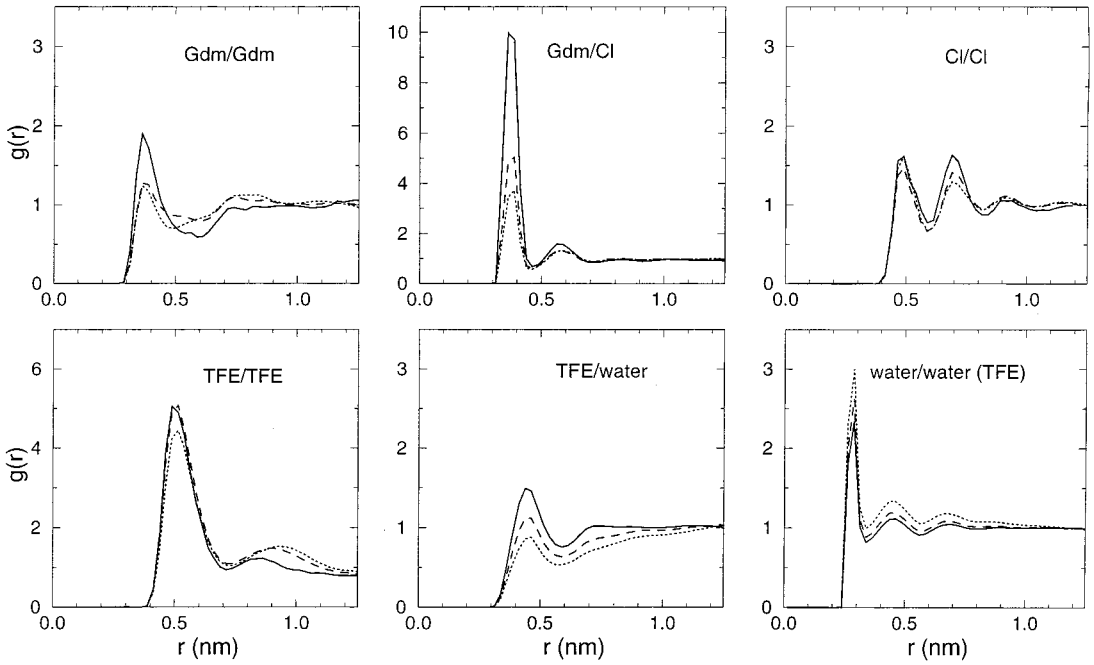

Figure 2. Radial distribution functions between selected pairs of species in GdmCl and TFE solutions of different concentrations. The solid line, dashed line, and dotted line correspond to successive increases in solution concentration.

TABLE 3: Radial Distribution Functions and Coordination Numbers[a]

		r_m (nm)					N_{ij}					
cosolvent	C_c (mol/L)	+/υ	−/υ	+/+	+/−	−/−	υ/υ	+/υ	−/υ	+/+	+/−	−/−
NaCl	0.55	0.34	0.36	0.51	0.35	0.59	4.6	6.1	6.6	0.1	0.2	0.2
NaCl	1.00	0.34	0.36	0.51	0.34	0.56	4.5	6.1	6.5	0.3	0.2	0.2
NaCl*	1.00	0.34	0.36	0.54	0.34	0.56	4.5	5.9	6.4	0.4	0.4	0.3
NaCl	1.58	0.34	0.36	0.51	0.34	0.56	4.5	5.9	6.3	0.4	0.4	0.4
NaCl	2.06	0.34	0.36	0.54	0.34	0.56	4.5	5.7	6.2	0.9	0.6	0.8
GdmCl	0.96	0.52	0.36	0.59	0.46	0.59	4.4	16.9	5.8	0.4	0.8	0.3
GdmCl	3.30	0.54	0.36	0.59	0.46	0.59	3.9	17.0	5.1	1.4	1.3	1.1
GdmCl	5.41	0.57	0.36	0.49	0.46	0.59	3.4	17.2	4.8	1.1	1.6	2.0
urea	0.95	0.58		0.61			4.5	22.9		0.7		
urea	5.31	0.56		0.61			4.0	15.0		3.7		
urea	7.80	0.54		0.61			3.7	11.7		5.4		
TFE	0.97	0.59		0.72			4.5	23.2		1.6		
TFE	2.67	0.59		0.73			4.3	15.0		5.0		
TFE	4.26	0.58		0.72			4.2	9.4		7.4		
TFE*	4.28	0.58		0.72			4.3	7.6		8.5		
TFE	13.82			0.72						12.7		

[a] r_m, position of the first minimum in the rdf; N_{ij}, the associated coordination number. For convenience, the properties for neutral solutes (urea and TFE) are listed under +/+ (solute around solute) and +/υ (water around solute). r_m for $\upsilon/\upsilon = 0.34$ nm for all solutions. $N_{\upsilon\upsilon} = 4.6$ in pure SPC/E water.

decrease in the number of waters in the hydration shells of Na^+ and Cl^- ions with concentration; the magnitude of which is in agreement with recent dielectric studies.[44] This was probably due to the formation of ion pairs indicated by the increased coordination numbers between both like and unlike ion pairs (see Table 3). Indeed, many complexes between sodium and chloride ions were observed especially at higher concentrations. In particular, Na_2Cl_2 complexes, with two chlorides in direct contact and stabilized by bridging sodium ions, were common. We are currently analyzing the significance of these complexes.

An increase in the number of Gdm−Cl and Cl−Cl ion pairs in the GdmCl solutions was observed. However, the rdfs for Gdm−Cl seem to indicate otherwise. This apparent contradiction is resolved when one considers that the rdfs indicate the propensity for association over and above the effect of increased numbers of such species. However, coordination numbers will naturally increase with concentration even if there is no significant interaction between the species involved. An *excess* coordination number of species *j* around species *i* may be defined as,

$$N_{ij}^{ex} = \rho_j \int_0^{r_m} 4\pi r^2 [g_{ij}(r) - 1]\, dr$$

where r_m is the position of the first minimum in the rdf between *i* and *j*. Excess coordination numbers are shown in Figure 3b as a function of solvent concentration and represent the excess or deficit of species *j* around species *i* compared to a random distribution. Clearly, the trends in Figure 3b more closely reflect those suggested by the rdfs (see Figure 2). The excess coordination numbers for Gdm−Cl ion pairs were invariant to increases in C_c, in contrast to the absolute coordination numbers, while the excess coordination numbers for Gdm−Gdm and Cl−Cl pairs increased and decreased, respectively. Analysis of relative orientations of guanidinium ions in the first coordination shell indicated that configurations in which the planes of the two ions are almost parallel were favored.

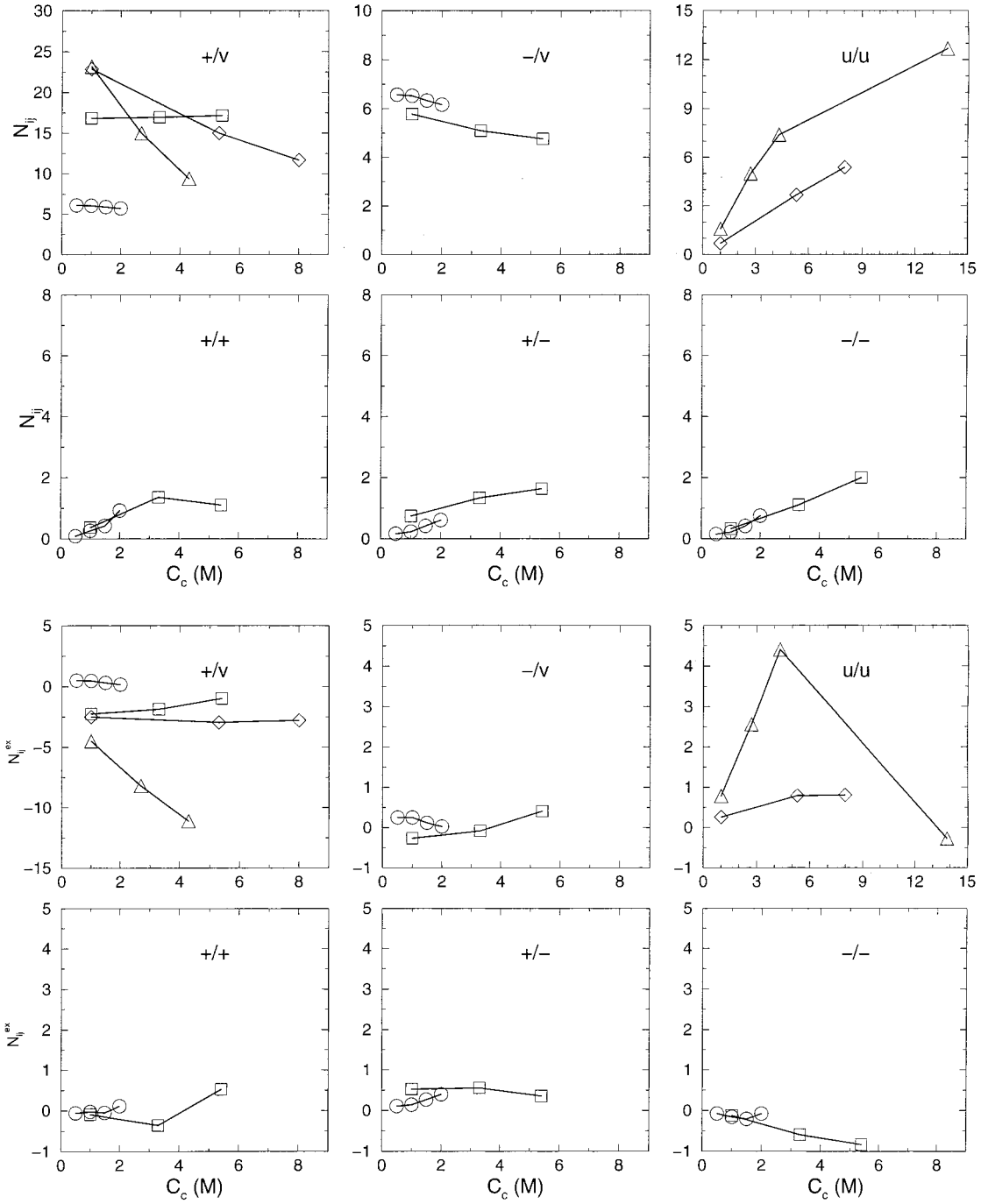

Figure 3. (a) Coordination numbers N_{ij} of different species are shown for NaCl (circles), GdmCl (squares), urea (diamonds), and TFE (triangles) solutions as a function of cosolvent concentration. (b) Excess coordination numbers N_{ij}^{ex} (see text for definition) are plotted for the same pairs of species as in (a).

The excess coordination number for urea−urea pairs increased slightly with increasing concentration indicating a tendency for the solutes to associate. However, an analysis of the relative orientations of urea molecules within the first coordination shell indicated that there was no particular preferred orientation. In fact, no evidence for the formation of long-lived linear, forked, or cyclic urea dimers was found. This is in contrast to other simulations.[18,19] However, the absence of any long-lived urea self-association is in agreement with previous NMR studies.[45]

Figure 3b indicates that the increased degree of association in TFE solutions at higher concentrations, which was accompanied by a decrease in the solvation of TFE by water molecules, was significantly greater than that expected by simple increases in concentration. This is in agreement with the experimentally observed clustering of TFE molecules in water,[46,47] which has been proposed as a possible mechanism for the stabilization of α-helices.[48] As is evident from Table 3, system size effects on coordination numbers were rather small, particularly for NaCl.

The effects of the cosolvents on the structure of water are discussed in detail elsewhere.[49] In summary, it was found that NaCl and GdmCl do not significantly affect the structure of water, while urea is a weak structure maker, and TFE is a strong structure maker. All effects increased with concentration.

C. Electroneutrality. The net charge in the vicinity of each cosolvent species, $Q(R)$, has been calculated based on (i) only ion−ion interactions (for salts), as well as (ii) cosolvent−cosolvent and cosolvent−water interactions (for salts and neutral

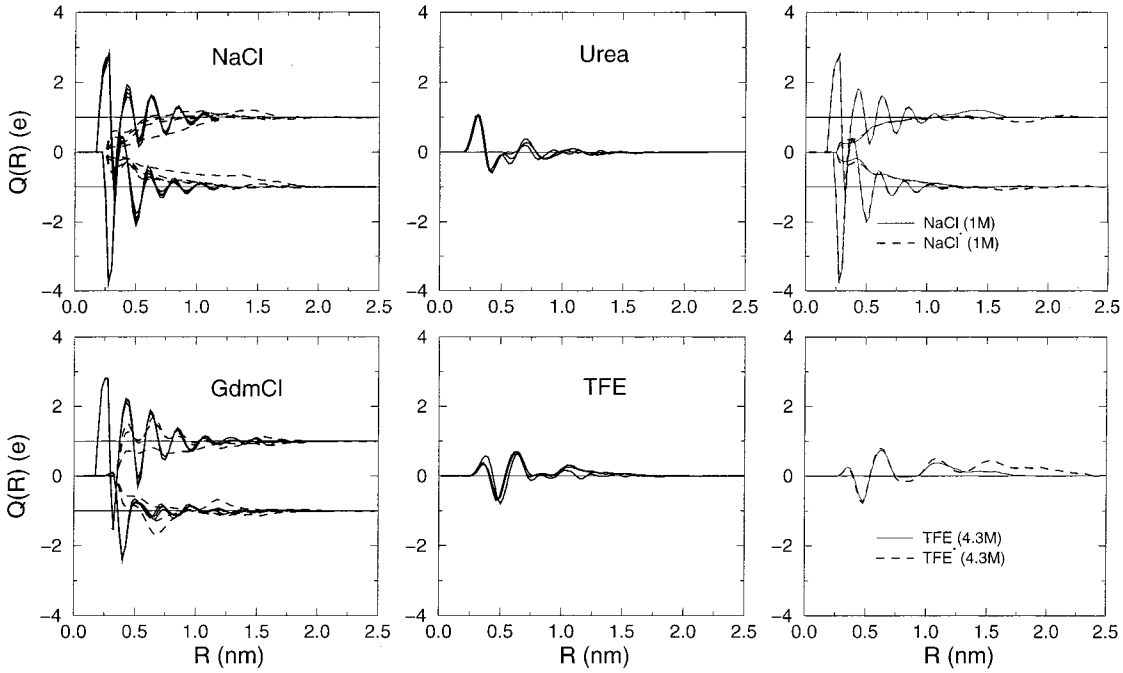

Figure 4. The net charge in the vicinity of each cosolvent species is plotted as a function of distance. For the salts, the net charge around the cation and anion is plotted separately, for all the concentrations reported here. The thin solid line indicates the net charge required for electroneutrality to be satisfied. The thick solid lines represent the net charge as calculated based on ion−ion as well as ion−water interactions, while the dotted lines indicate the same quantity calculated using only ion−ion interactions. The last two panels on the right indicate the effect of varying system size on NaCl (1 M) and TFE (4.3 M) solutions.

solutes). The results are shown in Figure 4. For the salts, the net charge as calculated by (i) varied appreciably with cosolvent concentration. The net charge tended to its expected value at shorter distances for the higher concentrations, in agreement with an increase in charge screening. In contrast, the net charge as calculated by (ii) exhibited strong oscillations for the salt solutions. For the NaCl solutions, there was a very small but systematic lowering of the peak heights with increasing concentration. It is probable that the observed oscillation was due to the alternating orientations of water molecules in the different solvation shells around the ion in question, the peak separation distance being close to the diameter of a water molecule (∼0.2 nm). The inclusion of water molecules resulted in charge neutralization at distances of 1.2 nm for NaCl and GdmCl solutions. Although this is close to $L/2$, a system size dependence can be ruled out as the larger NaCl system also displayed the same characteristics. In the case of the neutral solutes only method (ii) is appropriate. In contrast to the salts, the net charge around TFE or urea molecules displayed no regular oscillations. Both urea and TFE molecules were surrounded by an initial region of positive charge probably resulting from the presence of hydrogen atoms from nearby hydrogen bond donors. Figure 4 also illustrates the variation of the net charge with distance for NaCl and TFE solutions as a function of system size. While it appears that system size effects were negligible for NaCl, the TFE solution did display some differences, particularly at large distances.

D. Diffusion Constants. The diffusion constants of the various species in solution were calculated in order to study the effect of increasing concentration on their mobilities. The results are listed in Table 4 and displayed in Figure 5. In almost all the solutions studied, there was a clear retardation in diffusivities with increasing concentration. Our sodium chloride values compared reasonably well with other simulations in the literature.[42] While the calculated diffusivities of the Na^+ ions in NaCl solutions were in good agreement with experiment, the diffusivities of Cl^- ions were significantly smaller than the observed values.[12] This is probably due, at least in part, to the parameters used to describe the chloride ion interactions. Polarization effects (which have not been explicitly considered here) could play a significant role for this rather large anion, and consequently chloride ion parameters vary widely in the literature (σ (nm)/ϵ (kJ/mol): 0.4419/0.489,[50] 0.4864/0.168,[51] 0.4446/0.447,[52] 0.3884/4.558,[53] 0.3750/0.538[26]). The decrease in chloride ion diffusion constants with increasing concentration was significantly greater than experiment, but in good agreement with the results of Lyubartsev and Laaksonen.[14] The calculated diffusivities for urea and TFE compare fairly well with experimental values for low concentrations.[54,55] In fact, it is experimentally observed[56] that the diffusivity of urea solutions decreases linearly with increasing C_c for the range of concentrations considered here; a trend that was also observed in the calculated diffusivities as shown in Figure 5. At higher concentrations, the diffusion constants for TFE deviate from the experimental values primarily due to the incorrect value obtained for the diffusion constant of pure TFE.

An attempt to model changes in the diffusion constant of water was made using the approach of Hertz.[57] In this approach, the overall diffusion constant for water, D_v^{pred}, is divided into contributions from bulk water (D_v^{water}) and from hydration shell water associated with the cosolvent species. Hence,

$$D_v^{\text{pred}} = [D_+ N_{+/v} + D_- N_{-/v} + D_v^{\text{water}}(N_w - N_{+/v} - N_{-/v})]/N_w$$

where $N_{+/v}$ denotes the number of waters in the first hydration shell of the cations and D_+ is the simulated diffusion constant of the cations, etc. Hydration shells were defined as the distance to the first minimum in the appropriate rdf (see Table 3). The model was also applied to neutral cosolvent solutions, and the results are presented in Table 4. We note that for higher cosolvent concentrations, where sharing of waters between the hydration shells of two or more cosolvent molecules becomes

TABLE 4: Diffusion Coefficients of the Different Species in Solution[a]

		$D(\times 10^{-9}$ m^2/sec)							
cosolvent	C_c (mol/L)	D_v	D_v^{pred}	D_u	D_u^{exp}	D_+	D_+^{exp}	D_-	D_-^{exp}
none	0.00	2.73	2.73						
NaCl	ID						1.33[b]		2.03[b]
NaCl	0.55	2.39	2.55			1.2	1.28[c]	1.4	1.85[c]
NaCl	1.00	2.30	2.36			1.2	1.23[c]	1.1	1.78[c]
NaCl*	1.00	2.45	2.38			1.3		1.1	
NaCl	1.58	1.78	2.07			0.9		0.8	
NaCl	2.06	1.76	1.88			0.9	1.13[c]	0.7	1.66[c]
GdmCl	0.96	2.15	1.96			0.8		1.0	
GdmCl	3.30	1.31				0.4		0.5	
GdmCl	5.41	0.74				0.2		0.3	
urea	ID				1.38[d]				
urea	0.95	2.68	2.27	1.6	1.31[d]				
urea	5.31	2.17		1.2					
urea	7.80	2.13		1.0					
TFE	ID				1.13[e]				
TFE	0.97	2.44	2.01	1.1	1.01[e]				
TFE	2.67	2.30	1.19	1.0	0.81[e]				
TFE	4.26	2.04		0.9	0.68[e]				
TFE*	4.28	2.12		1.1	0.68[e]				
TFE	13.82			1.3	0.60[e]				

[a] D_v, D_u, D_+ and D_- denote diffusion coefficients of water, neutral cosolvent, cations, and anions, respectively. D^{exp} for pure water at 300 K = 2.3×10^{-9} m^2/sec (from ref 67). See text for definition of D_v^{pred}. ID = infinite dilution. [b] From ref 14. [c] From ref 12. [d] From ref 54. [e] From ref 55.

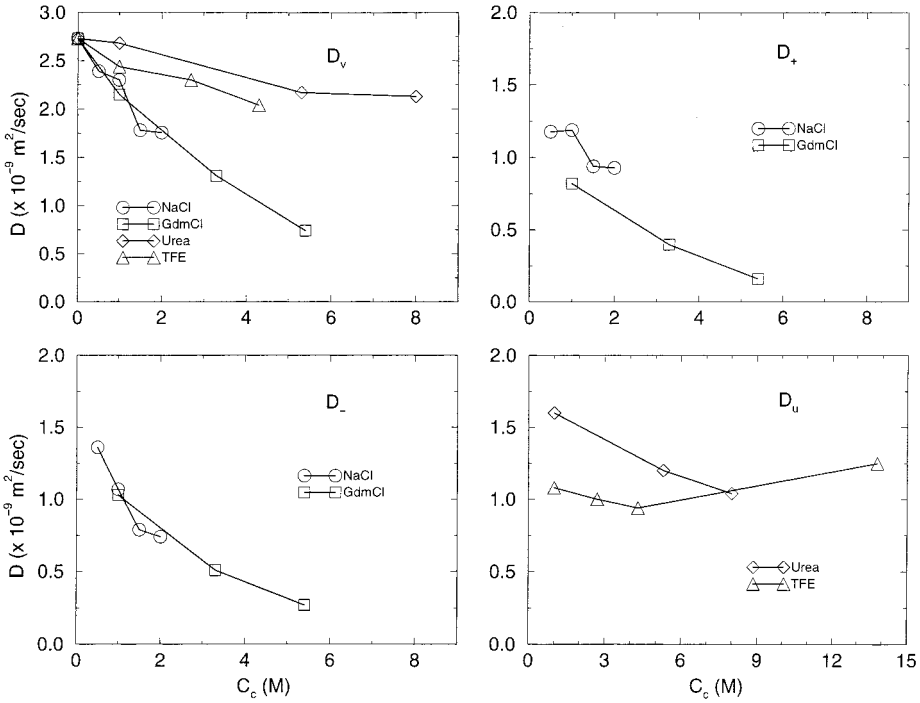

Figure 5. The diffusivities of different species in the cosolvent solutions are plotted as a function of cosolvent concentration. The diffusion constants of water, cations, anions, and the neutral solutes are shown in separate panels. The circles, squares, diamonds, and triangles represent solutions of NaCl, GdmCl, urea, and TFE, respectively.

more probable, the model breaks down giving values of $N_{+/v}$, etc., greater than the total number of waters in the system.

All cosolvents considered here diffused slower than water and hence the trends toward smaller water diffusion constants were reproduced. The predicted water diffusion constants in NaCl solutions were consistently higher than that observed, suggesting that one may need to include some fraction of waters associated with well-defined second solvation shells. This was not a problem for GdmCl solutions where too steep a decrease was predicted. However, the first solvation shell around the Gdm^+ ions was rather large, containing some 17 waters or so, which could explain the excessive decrease predicted. The predicted decreases for urea and TFE solutions were also larger than those observed in our simulations. Again, relatively large diffuse hydration shell definitions could explain these differences.

E. Residence Times. Residence times for water around different cosolvent species exhibited a range of effects with increasing concentrations (see Table 5 and Figure 6). The residence time, τ^r, of water around the neutral solutes (urea and TFE) was essentially independent of concentration. This is to be expected, since these solutes do not interact particularly strongly with water. Interestingly, τ^r for water around Na^+ ions, as well as that of water around Cl^- ions, did not vary

TABLE 5: Residence Times and Reorientational Relaxation Times[a]

		residence times			reorientational times		
cosolvent	C_c (mol/L)	$\tau^r_{+,v}$	$\tau^r_{-,v}$	$\tau^r_{+,-}$	$\tau^\mu_{+/v}$	$\tau^\mu_{-/v}$	$\tau^\mu_{+/+}$
none	0.00	4.8			5.0		
NaCl	0.55	16.1	16.3	52	19.9	11.4	
NaCl	1.00	16.9	16.2	53	20.8	13.1	
NaCl*	1.00	15.5	16.0	57	19.8	12.5	
NaCl	1.58	15.1	16.8	52	23.3	14.6	
NaCl	2.06	16.9	17.0	61	25.5	15.5	
GdmCl	0.96	13.7	17.3	86	16.5	14.2	72
GdmCl	3.30	24.0	25.3	66	34.7	24.0	178
GdmCl	5.41	46.5	35.5	89	56.7	42.3	306
urea	0.95	11.2		23	11.6		20
urea	5.31	12.0		25	18.1		59
urea	7.80	11.9		28	22.1		60
TFE	0.97	11.5		44	12.6		
TFE	2.67	11.1		38	17.2		
TFE	4.26	10.5		34	23.4		
TFE*	4.28	10.9		32	17.7		
TFE	13.82			27			

[a] $\tau^r_{+,v}$ and $\tau^r_{-,v}$ refer to residence times of water in the first hydration shells of cations and anions, respectively, while $\tau^r_{+,-}$ refers to that of anions around cations. $\tau^\mu_{+/v}$, $\tau^\mu_{-/v}$, and $\tau^\mu_{+/+}$ denote the reorientational relaxation times for water around cations, water around anions, and cations around cations, respectively. All reorientational times were calculated using first order Legendre polynomials. As before, the values for neutral solutes (as well as those for pure water) are listed under the values for water around cations. All times are in ps.

significantly with increasing concentration of NaCl, in agreement with other simulation results.[14] This is slightly unexpected as the number of ion pairs increased with concentration (see Table 3), but is supported by the fact that the coordination number for water around Na^+ and Cl^- ions changed only slightly with concentration (Table 3). The magnitude of the residence times for water around Na^+ and Cl^- were larger than early simulation studies,[40] but very similar to more recent results.[42]

Rather large effects were observed for the residence time of water around both Gdm^+ and Cl^- ions as the GdmCl concentration was increased. The significant increase in the residence times of water around Gdm^+ ions with concentration was not correlated with an increase in the coordination number for water around the guanidinium ions, which was independent of C_c. Note, however, the slight increase in the excess coordination number of water around the guanidinium ions as C_c was increased (see Figure 3b). It is also of interest to note that there was a sizable effect in the dependence of τ^r with concentration for water around chloride ions in GdmCl, but not for water around chloride ions in NaCl. Clearly, the solvation characteristics of the anion depended on the cation present in solution. The residence time and coordination number data indicate that, while there were fewer water molecules around the chloride ions in GdmCl, they were more tightly bound (much longer residence times). The residence times of anions around cations were statistically unreliable and specific trends could not be inferred from the present data.

In TFE solutions, τ^r for TFE around TFE decreased with increasing concentration. As there was more association at the higher concentrations, as indicated by the higher coordination numbers (see Table 3), this decrease in τ^r was probably a reflection of the fact that the solutions became more organic in nature with no strong directional bonds. On the other hand, a small increase in the residence times of urea molecules around other ureas was observed. This correlated with the slightly increased tendency for association of urea molecules at higher concentrations (see Table 3).

F. Reorientational Dynamics. The effects of increasing concentration on the reorientation of different species are tabulated in Table 5. For all the solutions studied here, the rotational relaxation times of water around a solute or ion (which were calculated for species in the first hydration shell only) were longer than that for water around water (5.0 ps), indicating that the water dynamics was considerably retarded. Also, not unexpectedly, the rotational motion was more hindered at higher concentrations. It is of interest to note that the rather diffuse Gdm^+ ion oriented the waters in its first hydration shell as

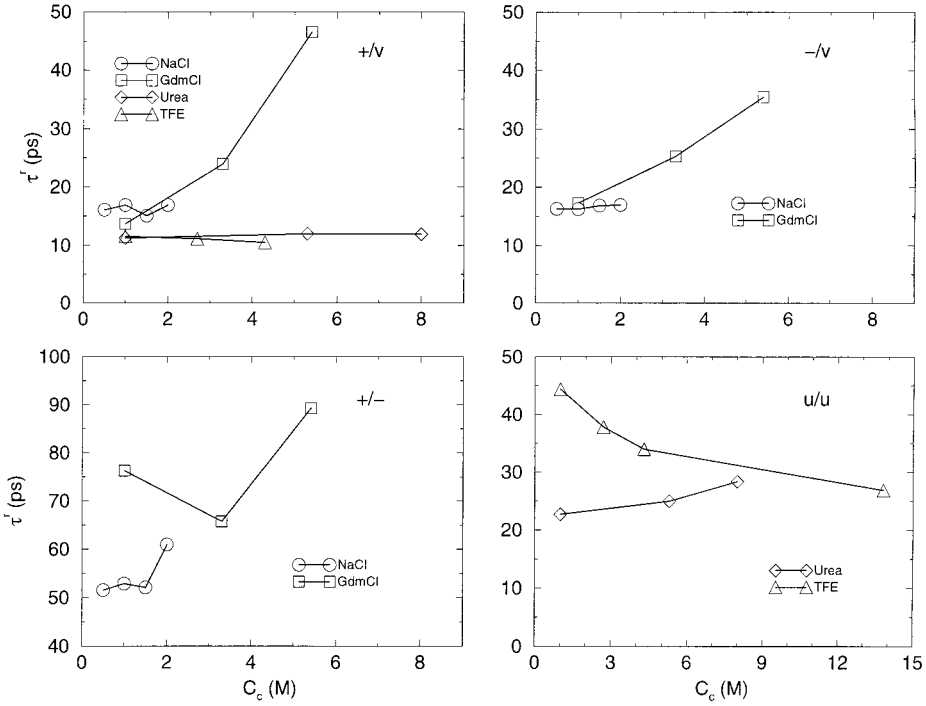

Figure 6. The residence times of one species around another are shown as a function of cosolvent concentration. The residence times for water around cations, water around anions, cations around anions, and neutral solutes around other neutral solutes are plotted separately.

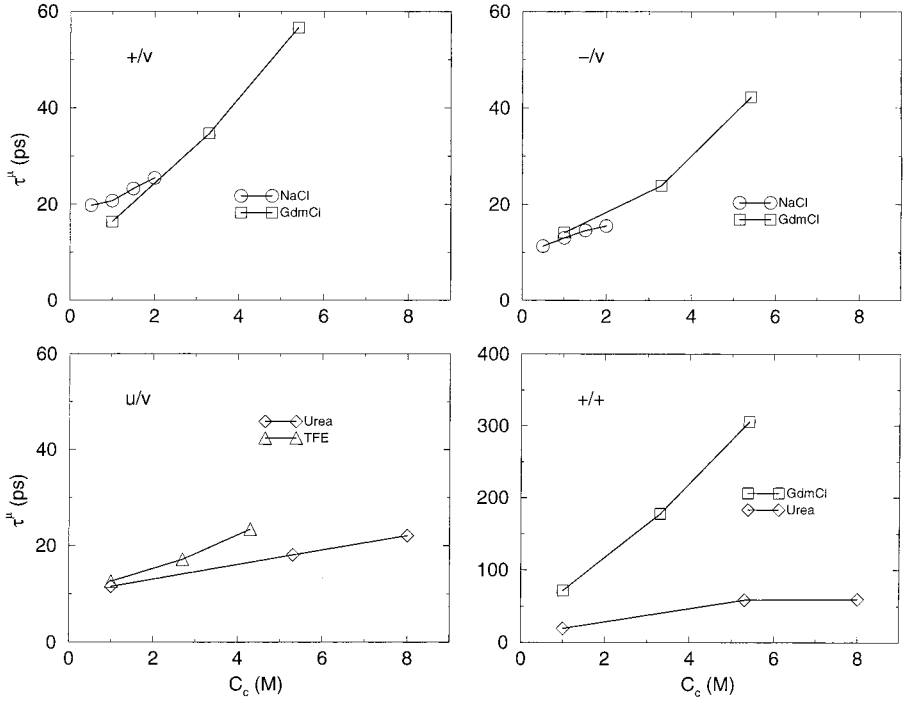

Figure 7. Reorientational times of different cosolvent species around other species are plotted against cosolvent concentration.

strongly as the much smaller Na^+ ion. Also, the chloride ions in both NaCl and GdmCl solutions appeared to affect the reorientational motion of water in much the same way. The reorientation of Gdm^+ ions around other Gdm^+ ions was very slow as can be seen from Figure 7. In general, our water orientational correlation times were larger than the infinite dilution NaCl values of Madden and Impey,[58] but in good agreement with previous results for urea solutions.[20]

G. Dielectric Properties. The dielectric constant decreased with increasing C_c in all solutions, with the possible exception of urea (see Figure 8). The variation of ϵ with concentration was markedly different for urea and GdmCl solutions, although they are both chaotropic agents.[59,60] While ϵ decreased and τ_D increased with concentration for GdmCl solutions, the dielectric properties of urea solutions remained almost unchanged. As expected, addition of a salt to water produced a decreased dielectric constant due to the restricted motion of water molecules in the first few solvation shells. In contrast, the addition of a polar solute such as urea actually increases the experimental dielectric constant.[61] There appeared to be no correlation between changes in individual reorientational times for water around neutral solutes or ions with cosolvent concentration, and changes in the dielectric response of the solution.

Table 6 lists the dielectric properties of the cosolvent solutions studied here along with the experimentally observed values where available. While the calculated value of ϵ for pure water agrees well with previous simulations,[62] it is rather low compared with the experimental value.[63] Consequently, comparison of the calculated absolute values with experimental values is rather difficult. To compare directly with experimental trends, a parameter $\delta\epsilon$ was defined as:

$$\delta\epsilon = \frac{\epsilon_{\text{solution}} - \epsilon_{\text{water}}}{\epsilon_{\text{water}} \cdot C_c}$$

which is related to the dielectric decrement.[64] The experimental trends in $\delta\epsilon$ with increasing concentration were reflected in the calculated values, except for the urea solutions for which the quantities were very small (see Table 6). The values of $\delta\epsilon$ obtained here for sodium chloride solutions were larger than previous simulation data,[11] although the force field parameters differ significantly between the two simulations. While qualitatively correct, the quantitative comparison between calculated and observed $\delta\epsilon$ values was complicated by the presence of

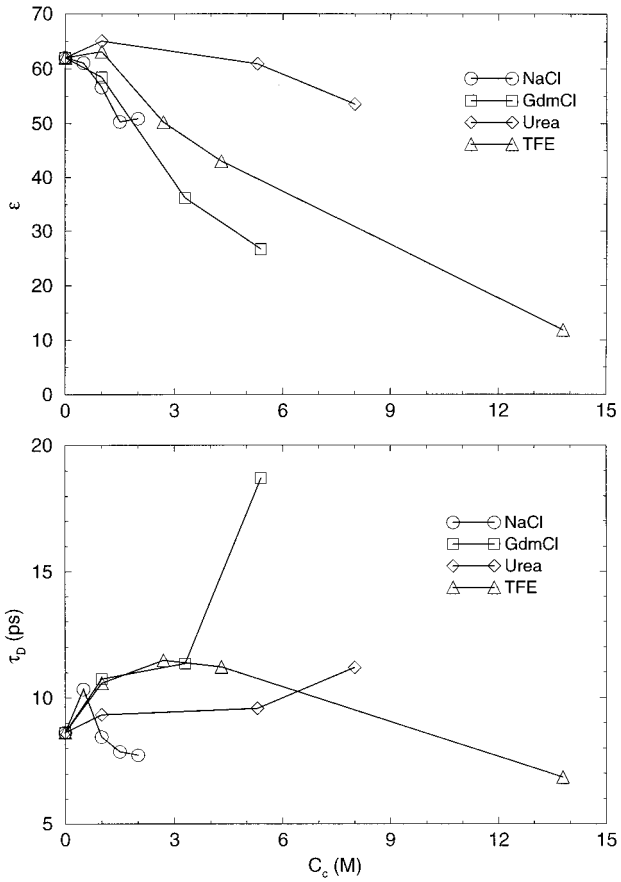

Figure 8. The dielectric constant, ϵ (top), and the dielectric relaxation time, τ_D (bottom) are plotted as a function of cosolvent concentration.

TABLE 6: Dielectric Properties of Solutions[a]

cosolvent	C_c (mol/L)	τ_D (ps)	τ_D^{exp} (ps)	ϵ	ϵ^{exp}	$\delta\epsilon$ (mol/L)$^{-1}$	$\delta\epsilon^{exp}$ (mol/L)$^{-1}$
none	0.00	8.6	8.2	62	78.5[b]		
NaCl	0.55	10.3	7.8	61	71.8[c]	0.0(1)	−0.155
NaCl	1.00	8.5	7.5	57	66.6[c]	−0.08(7)	−0.152
NaCl*	1.00	9.6	7.5	58	66.6[c]	−0.06(7)	−0.152
NaCl	1.58	7.9	7.3	50	62.0[c]	−0.12(4)	−0.133
NaCl	2.06	7.7	7.1	51	58.0[c]	−0.09(3)	−0.127
GdmCl	0.96	10.7	7.6	58	65.3[d]	−0.07(7)	−0.175
GdmCl	3.30	11.4	7.0	35	48.4[d]	−0.13(2)	−0.116
GdmCl	5.41	18.7		27		−0.10(1)	
urea	0.95	9.3		63	78.8[e]	0.02(7)	0.004
urea	5.31	9.6		61	91.7[e]	0.00(1)	0.032
urea	7.80	11.2		54	96.4[e]	−0.017(8)	0.029
TFE	0.97	10.6		63	75.5[f]	0.02(7)	−0.039
TFE	2.67	11.5		50	69.7[f]	−0.07(2)	−0.042
TFE	4.26	11.2		43	63.3[f]	−0.07(1)	−0.045
TFE*	4.28	14.0		47		−0.06(1)	
TFE	13.82	6.9		12	26.7[f]		

[a] $\delta\epsilon = (\epsilon_{solution} - \epsilon_{water})/(\epsilon_{water} \cdot C_c)$. Values in parentheses denote the error in the last digit, assuming the errors in the simulated ϵ values to be ± 3. τ_M is identical to the experimentally measured Debye relaxation time, τ_D. [b] From ref 63. [c] From ref 44. [d] From ref 68. [e] From ref 61. [f] From ref 69.

large errors associated with the calculated ϵ values. The error in the calculated dielectric constants was typically 5% and considerably longer simulations would be required to get more reliable estimates of dielectric properties. For NaCl solutions, the calculated values for τ_D decreased with increasing concentration, in agreement with experiment. However, the calculated relaxation times for GdmCl solutions suggested a strong retardation, while experiment actually measured a slight decrease in τ_D. System size effects on τ_D were observed for NaCl and TFE.

Conclusions

The properties of a series of cosolvent solutions have been investigated as a function of cosolvent concentration using molecular dynamics techniques. The results suggest that the observed trends in most properties were reproduced very well on a qualitative level, but significant quantitative differences from the experimental data were observed. Typically, a much larger change in many properties was observed in comparison with experiment. To a certain extent this is not surprising as the parameters have not been optimized to reproduce the data for cosolvent solutions. However, some of these quantitative differences were a direct consequence of inaccurate values for properties in the corresponding pure solutions.

A comparison of the simulated and experimental densities indicated significant deviations for the two ionic solutions toward systems with higher densities. In particular, the simulated densities of guanidinium chloride solutions were in poor agreement with experiment. Density changes in urea solutions were well reproduced. TFE density changes were also reasonably well reproduced but displayed a consistent deviation to lower density even though the simulated densities of pure water and pure TFE were excellent. System size effects were negligible.

The structure of the solutions, as measured by excess coordination numbers, did not vary with cosolvent concentration except for TFE and minor deviations for guanidinium chloride. For TFE solutions, the aggregation of TFE molecules increased with TFE concentration. However, this association did not appear to be the result of any specific interactions between TFE molecules as the residence times for TFE around TFE actually decreased with increasing concentration. Curiously, water coordination numbers for the sodium chloride solutions were essentially the values expected for a random distribution.

Results for the urea solutions were in reasonable agreement with experimental data. The urea model used here has been questioned due to the resulting low urea dimerization energy.[20] Correspondingly, no long-lived cyclic urea dimers were observed at any concentration during our simulations. However, one has to bear in mind that the urea force field is an effective force field which was developed to reproduce the solution properties of urea and not gas-phase properties.[24] Indeed, results for the diffusion constant of urea obtained here were more reasonable than that of a polarizable urea model which reproduced ab initio urea dimerization energies.[20]

Finally, oscillating regions of charge density were observed around the anions and cations present in solution. These oscillations appeared to involve water molecules located in successive solvation shells surrounding the respective ions. When considering the solvent and ions around a central ion the charge oscillations were shorter ranged than when considering just the ion atmosphere alone. These charge density fluctuations were independent of the system size used for the simulation and only varied slightly with salt concentration.

The data presented here suggest that most trends displayed by sodium chloride, guanidinium chloride, urea, and TFE solutions can be reasonably well reproduced in a qualitative manner. However, they also suggest that there is significant room for improvement in all of these models in order to reproduce the quantitative details of these solutions. We emphasize that this is a problem arising from the application of these models to describe cosolvent solutions, and not necessarily an indication of a poor initial parametrization. In addition, some of the cosolvent parameters were not derived for use with the SPC/E water model, or Ewald electrostatics, which could explain some of the discrepancies. Whether the required improvement can be obtained using better effective pair potentials, rather than an inclusion of explicit polarization effects, remains to be seen.

Acknowledgment. This project was partially supported by the Kansas Agricultural Experimental Station (Contribution No. 00-304-J). This material is based upon work supported by the National Science Foundation under Grant #EPS-9550487 and matching support from the State of Kansas, and DOE grant DE-FG02-99ER45764. Acknowledgment is made to the donors of the Petroleum Research Fund, administered by the ACS, for partial support of the research.

References and Notes

(1) von Hippel, P. H.; Schleich, T. *Acc. Chem. Res.* **1969**, *2*, 257−265.
(2) Franks, F.; Eagland, D. *C. R. C. Crit. Rev. Biochem.* **1975**, *3*, 165−219.
(3) Collins, K. D.; Washabaugh, M. L. *Q. Rev. Biophys.* **1985**, *18*, 323−422.
(4) Timasheff, S. N. *Curr. Opinion Struct. Biol.* **1992**, *2*, 35−39.
(5) Baldwin, R. L. *Biophys. J.* **1996**, *71*, 2056−2063.
(6) Cacace, M. G.; Landau, E. M.; Ramsden, J. J. *Q. Rev. Biophys.* **1997**, *30*, 241−277.
(7) Smith, P. E.; Pettitt, B. M. *J. Am. Chem. Soc.* **1991**, *113*, 6029−6037.
(8) Smith, P. E.; Pettitt, B. M. *Biopolymers* **1992**, *32*, 1623−1629.
(9) Smith, P. E.; Marlow, G. E.; Pettitt, B. M. *J. Am. Chem. Soc.* **1993**, *115*, 7493−7498.
(10) Smith, P. E. *J. Phys. Chem. B* **1999**, *103*, 525−534.
(11) Anderson, J.; Ullo, J.; Yip, S. *Chem. Phys. Lett.* **1988**, *152*, 447−452.

(12) Trullas, J.; Giro, A.; Padro, J. A. *J. Chem. Phys.* **1990**, *93*, 5177−5181.
(13) Hummer, G.; Soumpasis, D. M.; Neumann, M. *J. Phys.: Condens. Matter* **1994**, *6*, A141−A144.
(14) Lyubartsev, A. P.; Laaksonen, A. *J. Phys. Chem.* **1996**, *100*, 16410−16418.
(15) Kuharski, R. A.; Rossky, P. J. *J. Am. Chem. Soc.* **1984**, *106*, 5786−5793.
(16) Tanaka, H.; Nakanishi, K.; Touhara, H. *J. Chem. Phys.* **1985**, *82*, 5184−5191.
(17) Cristinziano, P.; Lelj, F.; Amodeo, P.; Barone, G.; Barone, V. *J. Chem. Soc., Faraday Trans. 1* **1989**, *85*, 621−632.
(18) Boek, E. S.; Briels, W. J. *J. Chem. Phys.* **1993**, *98*, 1422−1427.
(19) Hernandez-Cobos, J.; Ortega-Blake, I.; Bonilla-Marin, M.; Moreno-Bello, M. *J. Chem. Phys.* **1993**, *99*, 9122−9134.
(20) P. O. Åstrand, A. W.; Karlström, G. *J. Phys. Chem.* **1994**, *98*, 8224−8233.
(21) Berendsen, H. J. C.; Grigera, J. R.; Straatsma, T. P. *J. Phys. Chem.* **1987**, *91*, 6269−6271.
(22) Straatsma, T. P.; Berendsen, H. J. C. *J. Chem. Phys.* **1988**, *103*, 5876−5886.
(23) Jorgensen, W. L.; Tirado-Rives, J. *J. Am. Chem. Soc.* **1988**, *110*, 1657−1666.
(24) Duffy, E. M.; Kowalczyk, P. J.; Jorgensen, W. J. *J. Am. Chem. Soc.* **1993**, *115*, 9271−9275.
(25) van Buuren, A. R.; Berendsen, H. J. C. *Biopolymers* **1993**, *33*, 1159−1166.
(26) MacKerell, A. D., Jr.,; Bashford, D.; Bellott, M.; Dunbrack, R. L., Jr.; Field, M. J.; Fischer, S.; Gao, J.; Guo, H.; Ha, S.; Joseph, D.; Kuchnir, L.; Kuczera, K.; Lau, F. T. K.; Mattos, C.; Michnick, S.; Ngo, T.; Nguyen, D. T.; Prodhom, B.; Roux, B.; Schlenkrich, M.; Smith, J. C.; Stote, R.; Straub, J.; Wiorkiewicz-Kuczera, J.; Karplus, M. *FASEB Journal* **1992**, *6*, A143.
(27) van Gunsteren, W. F.; Berendsen, H. J. C. *Angew. Chem. Int. Ed. Engl.* **1990**, *29*, 992−1023.
(28) Ryckaert, J.-P.; Ciccotti, G.; Berendsen, H. J. C. *J. Comput. Phys.* **1977**, *23*, 327−341.
(29) de Leeuw, S. W.; Perram, J. W.; Smith, E. R. *Proc. R. Soc. London A.* **1980**, *373*, 27−56.
(30) Helfand, E. *J. Chem. Phys.* **1978**, *69*, 1010−1018.
(31) Loncharich, R. J.; Brooks, B. R.; Pastor, R. W. *Biopolymers* **1992**, *32*, 523−535.
(32) Helfand, E.; Wasserman, Z. R.; Weber, T. A. *Macromolecules* **1980**, *13*, 526−533.
(33) Neumann, M. *Mol. Phys.* **1983**, *50*, 841−858.
(34) Smith, P. E.; Brunne, R. M.; Mark, A. E.; van Gunsteren, W. F. *J. Phys. Chem.* **1993**, *97*, 2009−2014.
(35) Neumann, M. *J. Chem. Phys.* **1986**, *85*, 1567−1580.
(36) Hansen, J. P.; McDonald, I. R. *Theory of Simple Liquids*, 2nd ed.; Academic Press: London, 1986.
(37) Chandrasekhar, S. *Rev. Mod. Phys.* **1943**, *15*, 1−89.
(38) Smith, P. E.; van Gunsteren, W. F. *Mol. Simul.* **1995**, *15*, 233−245.
(39) Smith, P. E.; Pettitt, B. M. *J. Chem. Phys.* **1991**, *95*, 8430−8441.
(40) Impey, R. W.; Madden, P. A.; McDonald, I. R. *J. Phys. Chem.* **1983**, *87*, 5071−5083.
(41) Rey, R.; Guardia, E. *J. Phys. Chem.* **1992**, *96*, 4712−4718.
(42) Koneshan, S.; Rasaiah, J. C.; Lynden-Bell, R. M.; Lee, S. H. *J. Phys. Chem. B* **1998**, *102*, 4193−4204.
(43) Wallqvist, A.; Covell, D. G.; Thirumalai, D. *J. Am. Chem. Soc.* **1998**, *120*, 427−428.
(44) Buchner, R.; Hefter, G. T.; May, P. M. *J. Phys. Chem. A* **1999**, *103*, 1−9.
(45) Finer, E. G.; Franks, F.; Tait, M. J. *J. Am. Chem. Soc.* **1972**, *94*, 4424−4429.
(46) Kuprin, S.; Gräslund, A.; Ehrenberg, A.; Koch, M. H. J. *Biochem. Biophys. Res. Comm.* **1995**, *217*, 1151−1156.
(47) Hong, D. P.; Hoshino, M.; Kuboi, R.; Goto, Y. *J. Am. Chem. Soc.* **1999**, *121*, 8427−8433.
(48) Buck, M. *Q. Rev. Biophys.* **1998**, *31*, 297−355.
(49) Smith, P. E.; Chitra, R. *(in preparation)*.
(50) Chandrasekhar, J.; Spellmeyer, D. C.; Jorgensen, W. L. *J. Am. Chem. Soc.* **1984**, *106*, 903−910.
(51) Heinzinger, K. *Pure Appl. Chem.* **1985**, *57*, 1031−1042.
(52) Lybrand, T. P.; Kollman, P. A. *J. Chem. Phys.* **1985**, *83*, 2923−2933.
(53) Pettitt, B. M.; Rossky, P. J. *J. Chem. Phys.* **1986**, *84*, 5836−5844.
(54) Gostling, L. J.; Akeley, D. F. *J. Am. Chem. Soc.* **1952**, *74*, 2058−2060.
(55) Harris, K. R.; Newitt, P. J.; Derlacki, Z. J. *J. Chem. Soc., Faraday Trans.* **1998**, *94*, 1963−1970.
(56) Sorell, L. S.; Myerson, A. S. *AIChE J.* **1982**, *28*, 772−785.
(57) Hertz, H. G. Nuclear Magnetic Relaxation Spectroscopy. In *Water: A Comprehensive Treatise;* Franks, F., Ed.; Plenum: New York, 1973; Vol. 3, Ch. 7.
(58) Madden, P. A.; Impey, R. W. *Ann. New York Acad. Sci.* **1988**, *482*, 91−113.
(59) Wetlaufer, D. B.; Malik, S. K.; Stoller, L.; Coffin, R. L. *J. Am. Chem. Soc.* **1964**, *86*, 508−514.
(60) Frank, H. S.; Franks, F. *J. Chem. Phys.* **1968**, *48*, 4746−4757.
(61) Wyman, J., Jr. *J. Am. Chem. Soc.* **1933**, *55*, 4116−4121.
(62) Smith, P. E.; van Gunsteren, W. F. *J. Chem. Phys.* **1994**, *100*, 3169−3174.
(63) Pottel, R. Dielectric Properties. In *Water: A Comprehensive Treatise*; Franks, F., Ed.; Plenum: New York, 1973.
(64) Hasted, J. B. *Aqueous Dielectrics*. Chapman and Hall: London, 1973.
(65) Weast, R. C. *Handbook of Chemistry and Physics*; CRC Press: Cleveland, OH, 1975.
(66) Kawahara, K.; Tanford, C. *J. Biol. Chem.* **1966**, *241*, 3228−3232.
(67) Mills, R. *J. Phys. Chem.* **1973**, *77*, 685−688.
(68) Lileev, A. S.; Lyashchenko, A. K.; Yastremskii, P. S. *Russ. J. Phys. Chem.* **1985**, *59*, 978−981.
(69) Murto, J.; Heino, E. L. *Suomen Kemistilehti B* **1966**, *39*, 263−266.